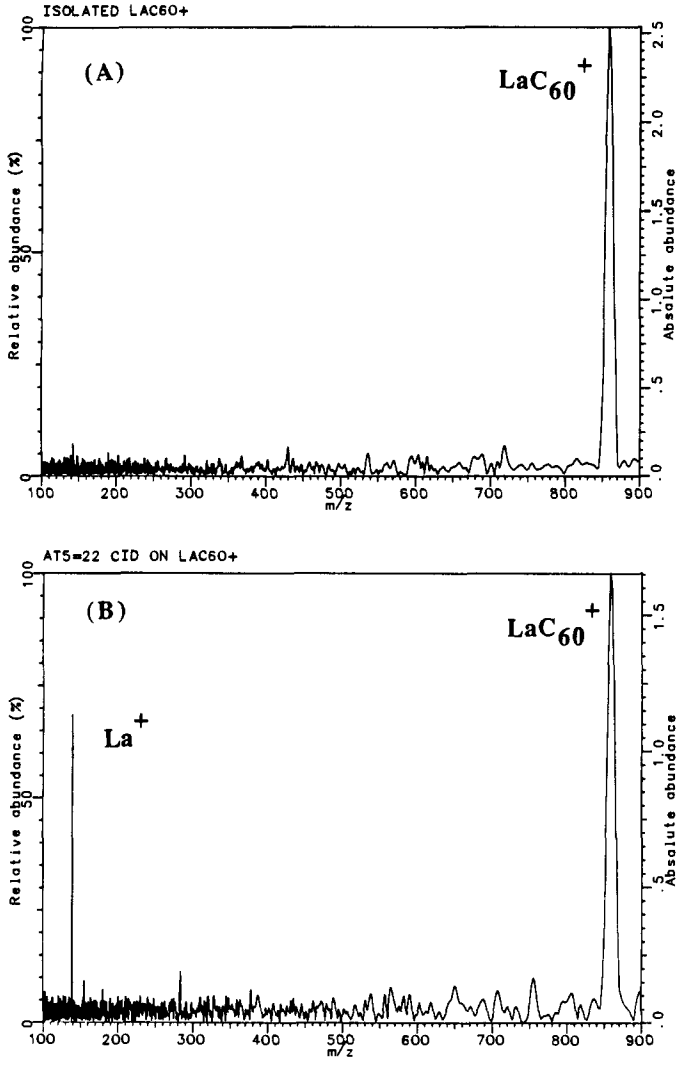

Figure 1. Plot of relative abundance vs m/z: (A) isolated LaC_{60}^+; (B) collision-induced dissociation of LaC_{60}^+ (105 eV Laboratory, 4.7 eV center of mass energy) yielding La^+.

7.46 eV, IP(VO) = 7.23 eV (Weisshaar, J. C., private communication) and IP(La) = 5.577 eV, the CID results indicate IP(Fe, Co, Ni, Cu) > IP(C_{60}) ~ IP(Rh) > IP(VO, La), which is in agreement with a recently reported value of IP(C_{60}) = 7.61 ± 0.11 eV.[17] Furthermore, these results provide strong support for internally bound "egg shell" MC_{60}^+ species (particularly for M = La) reported earlier grown in a supersonic expansion, since these latter species are highly stable and lose C_2 molecules when sufficiently activated. In direct contrast, the externally bound isomers, presumably always formed by adding the metal to the preformed C_{60}, require relatively little activation energy to cleave the metal from the complex, leaving an intact C_{60} species. Although the type of activation used in the current study (collisional) and that reported in the previous study (photoexcitation) can yield different fragmentation processes,[18] it is likely that some metal loss would be observed for an externally bound complex regardless of the method of excitation employed.

Studies are underway to synthesize other members of this new family of ions and to characterize their subsequent chemistry with other reagent gases. It should be possible to synthesize virtually any metal ion–C_{60} complex, as well as an endless variety of ligated metal ion–C_{60} complexes, in the gas phase. Determination of the M^+–C_{60} bond energies will also be possible by monitoring ligand-exchange reactions using reference ligands.

Acknowledgment is made to the Division of Chemical Sciences in the United States Department of Energy (DE-FG02-87ER13766) and to the National Science Foundation (CHE-8920085) for their support. In addition, the authors thank J. C. Gunderson and Professors D. Ben-Amotz and B. Kahr for providing the fullerene sample and for their helpful discussions.

Surface Electrostatics, Reduction Potentials, and the Internal Dielectric Constant of Proteins

Karla K. Rodgers and Stephen G. Sligar*

Departments of Chemistry Biochemistry, and Biophysics, and The Beckman Institute for Advanced Science and Technology University of Illinois at Urbana-Champaign Urbana, Illinois 61801

Received July 22, 1991

Electrostatic contributions by surface charges are presumed to play important roles in dictating the affinity and selectivity of numerous protein–macromolecule and protein–small molecule interactions. Although numerous modeling and theoretical efforts have attempted to predict the detailed electrostatic fields in and around globular proteins,[1] there have been only a few systematic efforts to experimentally map the electrostatic potential surface of a protein in solution and correlate this with simplified theories.[1h] In this communication we demonstrate that site-directed mutagenesis of surface charges together with high-resolution electrochemical measurements can be used to quantitate the boundary-value electrostatic potentials of soluble proteins.

Prosthetic group reduction potentials[2] and amino acid side chain ionization constants can be affected by surface-charged residues.[3] Here we show that precise measurement of the shift in the reduction potential for a heme prosthetic group upon alteration of surface charge can be used to test the validity of theoretical calculations of macromolecular electrostatic fields and, in a simple two-continuum dielectric model, to estimate the effective bulk internal dielectric constant of a protein. By using amino acid replacements at numerous sites on the surface, we find that a single distance-dependent dielectric will not fit experimental data, but rather the detailed shape of the macromolecule must be taken into account.

We have chosen rat liver cytochrome b_5 for these investigations, since previous studies have shown that the protein is structurally rigid to surface mutations.[4] The heme redox potential was measured by direct electrochemical methods using a cysteine-modified gold working electrode.[5] For these investigations we

(17) Zimmerman, J. A.; Eyler, J. R.; Bach, S. B. H.; McElvaney, S. W. *J. Chem. Phys.* **1991**, *95*, 3267.
(18) Franchetti, V.; Freiser, B. S.; Cooks, R. G. *Org. Mass Spectrom.* **1978**, *13*, 106.

* To whom correspondence should be addressed.

(1) (a) Mathew, J. B. *Annu. Rev. Biophys. Biophys. Chem.* **1985**, *14*, 387–417. (b) Honig, B. H.; Hubbell, W. L.; Flewelling, R. F. *Annu. Rev. Biophys. Biophys. Chem.* **1986**, *15*, 163–193. (c) Schoefer, M.; Froemmel, C. *J. Mol. Biol.* **1990**, *216*, 1045–1066. (d) Bashford, D. *Curr. Opin. Struct. Biol.* **1991**, *1*, 175–184. (e) Harvy, S. C. *Proteins* **1989**, *5*, 78–92. (f) Sharp, K. A.; Honig, B. *Annu. Rev. Biophys. Biophys. Chem.* **1990**, *19*, 301–332. (g) Davis, M. E.; McCammon, J. A. *Chem. Rev.* **1990**, *90*, 509–521. (h) Bashford, D.; Karplus, M. *Biochemistry* **1990**, *29*, 10219–10225. (i) Karshikov, A. D.; Engh, R.; Bode, W.; Atanasov, B. P. *Eur. Biophys. J.* **1989**, *17*, 287–297.
(2) (a) Smith, H. T.; Staudenmeyer, M.; Millett, F. *Biochemistry* **1977**, *16*, 4971–4974. (b) Reid, L. S.; Mauk, M. R.; Mauk, A. G. *J. Am. Chem. Soc.* **1984**, *106*, 2182–2185. (c) Caffrey, M. S.; Cusanovich, M. A. *Arch. Biochem. Biophys.* **1991**, *285*, 227–230.
(3) Sternberg, M. J. E.; Hays, F. R. F.; Russell, A. J.; Thomas, P. G.; Fersht, A. R. *Nature* **1987**, *330*, 86–88.
(4) (a) Rodgers, K. K.; Pochapsky, T. C.; Sligar, S. G. *Science* **1988**, *240*, 1657–1659. (b) Rodgers, K. K.; Sligar, S. G. *J. Mol. Biol.*, in press.
(5) (a) Di Gleria, K.; Hill, H. A. O.; Lowe, V. J.; Page, D. J. *J. Electroanal. Chem.* **1986**, *213*, 333–338. (b) Hill, H. A. O.; Lawrance, G. A. *J. Electroanal. Chem.* **1989**, *270*, 309–318. (c) Bagby, S.; Barker, P. D.; Guo, L.-H.; Hill, H. A. O. *Biochemistry* **1990**, *29*, 3213–3219.

0002-7863/91/1513-9419$02.50/0

Table I. Reduction Potentials of Cytochrome b_5 Variants

protein[a]	$E°'$ (mV)[b,c] (vs NHE)	$k°$ (cm/s)[b] ($\times 10^4$)
wild type	−7	4
E11Q	−7	3
E37Q	−5	4
E56Q	−3	4
E44Q	−1	4
E48Q	+1	4
D66S	+1	5
D60N	+3	6
E44Q, E48Q	+5	4
E43Q, E44Q	+7	3
E44Q, E48Q, D60N	+13	4
D66K	+5	14
E44K	+1	16
Q13E	−9	2
S64D	−13	0.9

[a] The method of site-directed mutagenesis of cytochrome b_5 has been reported previously.[4,17] [b] The errors in measurement for these determinations were ±1 mV for $E°'$ and ±3 × 10^{-4} cm/s for $k°$ corresponding to the mean ± 1 standard deviation from at least three independent measurements. [c] The reduction potentials were determined by differential pulse voltammetry. The solutions were in Bis-Tris/HCl, 2 mM L-cysteine, with NaCl to μ = 0.1 M, pH 7.0.

focus only on the effect of distant surface-charge mutations on this potential. Several other factors that can contribute to the absolute reduction potential energy of metalloprotein systems are the polarity of the heme environment,[6] the nature of the axial ligands,[7] and the detailed electronic structure of the heme macrocycle.[8]

The reduction potentials measured for the wild-type protein and the various surface-charge mutations are listed in Table I. The value obtained for the wild-type protein corresponds closely with previously reported measurements.[8a,9] Mutations include a series of substitutions of negatively charged residues with neutral side chains at single and multiple sites. Also, the polarities of two negatively charged residues were reversed to give positive charges, while two neutral residues were replaced with negative charges. Most of the shifts in reduction potentials of the various surface-charge mutations versus the wild-type protein are in the direction expected for the sign of the change in surface charge, indicating that the effect of surface-charge mutation on the reduction potential is mainly through electrostatic interactions.

Several theoretical models in the treatment of electrostatic interactions in proteins have been developed. Perhaps the most straightforward are macroscopic continuum dielectric models. First approximations of this method utilized a low-dielectric sphere to represent the protein present in a high-dielectric medium.[1f,10] Refinement includes the introduction of finite difference techniques,[11] which takes into account the complex shape of macromolecules. Using a finite difference solution of the Poisson–Boltzmann equation, we have analyzed the effect of surface-charge mutation on the experimentally determined reduction potentials of cytochrome b_5. The relative reduction potential of the charge mutations versus the wild-type protein is presented in Figure 1. An excellent agreement between the calculated and the experimental values is found if a dielectric constant of 2–4 is used for the protein interior. This simplified theory is also able to account for multiple mutations and for substitutions which reverse the polarity of the side chains.

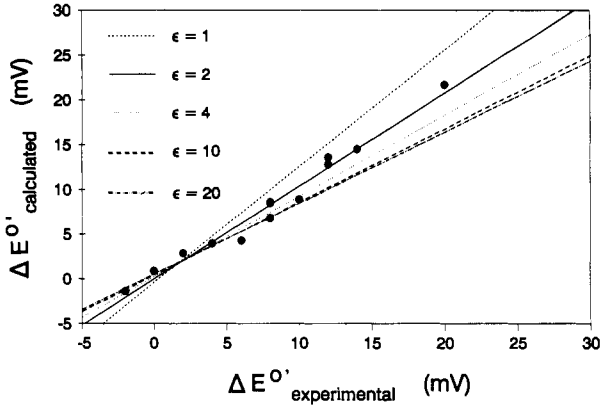

Figure 1. Comparison of the experimentally determined difference between mutant and wild-type redox potentials with five separate calculations using a two-continuum model with different values for the protein dielectric constant. The potentials were calculated, using the bovine cytochrome b_5 coordinates (Brookhaven Data Bank), for the residues in the native protein using a differential charge assignment of +1 for the heme iron. In each determination a dielectric constant of 80 was assigned to the solvent at an ionic strength of 0.1 M, a probe radius of 1.4 Å was used in determination of the solvent-exposed surface, and a Stern layer of 1.4 Å was used as determined from the average of the radii of Na^+ and Cl^- ions. Focusing, as well as rotational averaging of five separate grid orientations, used the program DELPHI (Biosym Technologies) according to the method of Gilson et al.[11c] The result for the charge mutation S64D was not included, as it is likely that introduction of a negatively charged residue in this position would result in structural changes due to electrostatic repulsion with a heme propionate group.[18]

Heterogeneous electron transfer rate constants at the modified gold electrode surface were also measured[12] and are shown in Table I. A previously reported value of 8.13 × 10^{-7} cm^2/s for the diffusion coefficient of bovine cytochrome b_5[13] was utilized to calculate the heterogeneous rate constants ($k°$) acquired from a series of cyclic voltammograms at various scan rates.[14] The mutations in which negative charges were eliminated resulted roughly in the same $k°$ as wild type within experimental error. However, the D66K and E44K mutations in which a positive charge was introduced near the exposed heme edge resulted in a greater than 3-fold increase in $k°$. Likewise introduction of a negative charge near the heme group (S64D) yielded a 3-fold decrease. The decrease in $k°$ upon increasing negative charge appears to involve the region around the exposed heme edge, as the mutation Q13E, positioned well away from the heme group, shows the similar $k°$ as the wild-type protein. Apparently, as cytochrome b_5 becomes more negatively charged, electrostatic repulsion increases between the protein and electrode, indicating that the electrode is negatively charged under the conditions of these experiments. The site of cytochrome b_5 that interacts with the electrode most likely involves the region surrounding the exposed heme edge, as the mutations demonstrating altered $k°$'s are positioned in this area of the protein surface. These residues surrounding the heme crevice of native cytochrome b_5 have been

(6) (a) Kassner, R. J. *Proc. Natl. Acad. Sci. U.S.A.* **1972**, *69*, 2263–2267. (b) Stellwagen, E. *Nature* **1978**, *275*, 73–74.

(7) (a) Marchon, J.-C.; Mashiko, T.; Reed, C. A. In *Electron Transport and Oxygen Utilization*; Ho, C., Ed.; Elsevier: North-Holland, New York, 1982; pp 67–73. (b) Sligar, S. G.; Egeberg, K. D.; Sage, J. T.; Morikis, D.; Champion, P. M. *J. Am. Chem. Soc.* **1987**, *109*, 7896–7897. (c) Raphael, A. L.; Gray, H. B. *J. Am. Chem. Soc.* **1991**, *113*, 1038–1040.

(8) (a) Martinis, S. A.; Sotiriou, C.; Chang, C. K.; Sligar, S. G. *Biochemistry* **1989**, *28*, 879–884. (b) Reid, L. S.; Lim, A. R.; Mauk, A. G. *J. Am. Chem. Soc.* **1986**, *108*, 8197–8201.

(9) (a) Reid, L. S.; Taniguchi, V. T.; Gray, H. B.; Mauk, A. G. *J. Am. Chem. Soc.* **1982**, *104*, 7516–7519. (b) Walker, F. A.; Emrick, D.; Rivera, J. E.; Hanquet, B. J.; Buttlaire, D. H. *J. Am. Chem. Soc.* **1988**, *110*, 6234–6240.

(10) (a) Tanford, C.; Kirkwood, J. G. *J. Am. Chem. Soc.* **1957**, *79*, 5333–5339. (b) Shire, S. J.; Hanania, G. I. H.; Gurd, F. R. N. *Biochemistry* **1974**, *13*, 2967–2974. (c) Matthew, J. B.; Gurd, F. R. N. *Methods Enzymol.* **1986**, *130*, 413–436.

(11) (a) Warwicker, J.; Watson, H. C. *J. Mol. Biol.* **1982**, *157*, 671–679. (b) Klapper, I.; Hagstrom, R.; Fine, R.; Sharp, K.; Honig, B. *Proteins: Struct., Funct., Genet.* **1986**, *1*, 47–59. (c) Gilson, M.; Sharp, K.; Honig, B. *J. Comput. Chem.* **1987**, *9*, 327–335. (d) Gilson, M.; Honig, B. *Nature* **1987**, *330*, 84–86. (e) Bashford, D.; Karplus, M. *J. Mol. Biol.* **1988**, *203*, 507–510. (f) Rashin, A. *J. Phys. Chem.* **1990**, *94*, 1725–1733.

(12) (a) Nicholson, R. S. *Anal. Chem.* **1965**, *37*, 1351–1355. (b) Bard, A. J.; Faulkner, L. R. *Electrochemical Methods*; Wiley: New York, 1980; pp 230–231.

(13) Strittmatter, P. *J. Biol. Chem.* **1960**, *235*, 2492–2487.

(14) Hill, H. A. O.; Whitford, D. *J. Electroanal. Chem.* **1987**, *235*, 153–167. (b) Barker, P. D.; Di Gleria, K.; Hill, H. A. O.; Lowe, V. J. *Eur. J. Biochem.* **1990**, *190*, 171–175.

previously shown experimentally to have a major role in the specificity of association with other heme proteins, indicating that cytochrome b_5 interacts with the electrode in an orientation similar to its association with other redox proteins, such as cytochrome *c*.[4]

In conclusion, although individual surface charges on a redox protein appear to have a relatively minor role in the determination of the reduction potential, it is apparent that the summed distribution pattern of surface charges can make a significant contribution. The excellent quantitative agreement between experimentally determined potential surfaces and the results of a simplified continuum dielectric model suggests that a protein interior can be approximated by a macroscopic dielectric constant in many instances. Our derived value for this parameter of between 2 and 4 is consistent with earlier estimates from fluorescence energy transfer[15] and the high-frequency dielectric of organic liquids[1f] and lower than that estimated for the hydrated pocket of myoglobin.[16]

Acknowledgment. We thank Dr. Larry Faulkner for helpful discussions and Dr. David Conrad for advice on experimental parameters. This work was supported by National Institutes of Health Grants GM31756 and GM33775, the Materials Research Laboratory supported by NSF DMR8920538, and the Biotechnology Research and Development Corporation.

Supplementary Material Available: Figures of differential pulse and cyclic voltammograms and a description of electrochemical parameters and conditions used (3 pages). Ordering information is given on any current masthead page.

(15) Stryer, L. *J. Mol. Biol.* **1965**, *13*, 482–495.
(16) Macgregor, R. B.; Weber, G. *Nature* **1986**, *319*, 70–73.
(17) Beck von Bodman, S.; Schuler, M. A.; Jollie, D. R.; Sligar, S. G. *Proc. Natl. Acad. Sci. U.S.A.* **1986**, *83*, 9443–9447.
(18) Argos, P.; Mathews, F. S. *J. Biol. Chem.* **1975**, *250*, 747–751.

Synthesis and Structure of $W(PMe_3)_4(Te)_2$: The First Transition-Metal Complex with a Terminal Tellurido Ligand

Daniel Rabinovich and Gerard Parkin*

Department of Chemistry, Columbia University
New York, New York 10027

Received July 26, 1991

In view of the current interest in both the bonding and reactivity of complexes that contain metal–ligand multiple bonds,[1,2] we are presently investigating synthetic methods for such complexes in which the ligands are derived from the heavier members of the main group elements. Furthermore, because of the increased tendency of the heavier elements to bridge two or more metal centers,[3-5] the synthesis of complexes that contain *terminal* metal–ligand multiple bonds is even more challenging. Here we report the synthesis and chracterization of *trans*-$W(PMe_3)_4(Te)_2$, a complex which, to our knowledge, contains the first *terminal* transition metal–tellurium double bond.

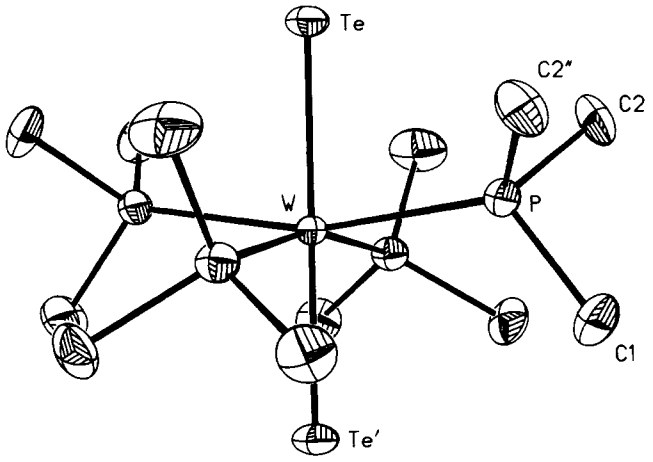

Figure 1. ORTEP drawing of *trans*-$W(PMe_3)_4(Te)_2$. Selected bond lengths (Å) and angles (deg): W–Te = 2.596 (1), W–P = 2.508 (2); Te–W–Te′ = 180.0, Te–W–P = 82.1 (1), Te′–W–P = 97.9 (1), P–W–P* = 91.1 (1), 164.2 (1) (an asterisk indicates other phosphorus atoms).

We have recently reported that the bis(sulfido) complex *trans*-$W(PMe_3)_4(S)_2$ may be readily obtained by the reaction of $W(PMe_3)_4(\eta^2\text{-}CH_2PMe_2)H$ with H_2S, accompanied by elimination of dihydrogen.[6] Although the corresponding reaction with H_2Te may provide a route to the analogous (bis)tellurido complex *trans*-$W(PMe_3)_4(Te)_2$, the instability of H_2Te[7] limits the convenience of such a method. However, we have found that the reaction between $W(PMe_3)_4(\eta^2\text{-}CH_2PMe_2)H$ and elemental tellurium provides a straightforward synthesis of *trans*-$W(PMe_3)_4(Te)_2$. Thus, a solution of $W(PMe_3)_4(\eta^2\text{-}CH_2PMe_2)H$ in pentane reacts smoothly with elemental tellurium at room temperature to give red-brown *trans*-$W(PMe_3)_4(Te)_2$ in good yield (eq 1).[8] The molecular structure of *trans*-$W(PMe_3)_4(Te)_2$ has

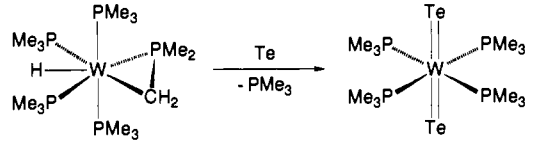

(1)

been determined by X-ray diffraction, as shown in Figure 1.[9] Of particular significance, the W=Te bond length [2.596 (1) Å] is noticeably shorter than those observed for a variety of other complexes that contain W–Te single bonds, typically in the range 2.68–2.88 Å.[10] Furthermore, electronic considerations of the

(1) Nugent, W. A.; Mayer, J. M. *Metal-Ligand Multiple Bonds*; Wiley-Interscience: New York, 1988.
(2) Harlan, E. W.; Holm, R. H. *J. Am. Chem. Soc.* **1990**, *112*, 186–193 and references therein.
(3) For studies concerned with metal–ligand multiple bonding of the heavier elements see: (a) Herrmann, W. A. *Angew. Chem., Int. Ed. Engl.* **1986**, *25*, 56–76. (b) Compton, N. A.; Errington, R. J.; Norman, N. C. *Adv. Organomet. Chem.* **1990**, *31*, 91–182. (c) Hitchcock, P. B.; Lappert, M. F.; Leung, W.-P. *J. Chem. Soc., Chem. Commun.* **1987**, 1282–1283. (d) Cowley, A. H.; Barron, A. R. *Acc. Chem. Res.* **1988**, *21*, 81–87. (e) Cowley, A. H.; Pellerin, B.; Atwood, J. L.; Bott, S. G. *J. Am. Chem. Soc.* **1990**, *112*, 6734–6735. (f) Straus, D. A.; Grumbine, S. D.; Tilley, T. D. *J. Am. Chem. Soc.* **1990**, *112*, 7801–7802.
(4) (a) Do, Y.; Holm, R. H. *Inorg. Chim. Acta* **1985**, *104*, 33–40. (b) Vahrenkamp, H. *Angew. Chem., Int. Ed. Engl.* **1975**, *14*, 322–329. (c) Rice, D. A. *Coord. Chem. Rev.* **1978**, *227*, 199–227.
(5) (a) Ansari, M. A.; Ibers, J. A. *Coord. Chem. Rev.* **1990**, *100*, 223–266. (b) Kanatzidis, M. G. *Comments Inorg. Chem.* **1990**, *10*, 161–195.
(6) Rabinovich, D.; Parkin, G. *J. Am. Chem. Soc.* **1991**, *113*, 5904–5905.
(7) H_2Te decomposes above 0 °C. Greenwood, N. N.; Earnshaw, A. *Chemistry of the Elements*; Pergamon Press: New York, 1986.
(8) A solution of $W(PMe_3)_4(\eta^2\text{-}CH_2PMe_2)H$ (2.95 g, 5.23 mmol) in pentane (20 mL) was stirred with Te powder (1.20 g, 9.40 mmol) for 20 h at room temperature, resulting in the precipitation of *trans*-$W(PMe_3)_4(Te)_2$ as a red-brown solid. The mixture was filtered and the product extracted into benzene (ca. 30 mL) and filtered, and the solvent was removed under reduced pressure giving pure *trans*-$W(PMe_3)_4(Te)_2$ (1.37 g). The residue (0.89 g) is sufficiently pure for further reactions. Overall yield ca. 65%. Elemental analysis calculated for $W(PMe_3)_4(Te)_2$: C, 19.4, H. 4.9. Found: C, 19.4, H, 4.6. NMR data for *trans*-$W(PMe_3)_4(Te)_2$ (in C_6D_6): ^1H δ 1.91, virtual triplet, "J_{P-H}" = 2.8 Hz; $^{13}C\{^1H\}$ δ 33.6, multiplet, "J_{P-C}" = 15 Hz; $^{31}P\{^1H\}$ (relative to H_3PO_4) δ −51.2, s, $^1J_{W-P}$ = 238 Hz (^{183}W, $I = {}^1/_2$, 14.27%), $^2J_{P-Te}$ = 17 Hz (^{125}Te, $I = {}^1/_2$, 6.99%); $^{125}Te\{^1H\}$ (relative to Me_2Te) δ 958, quintet, $^2J_{P-Te}$ = 17 Hz, $^1J_{Te-W}$ = 190 Hz (^{183}W, $I = {}^1/_2$, 14.27%). Note: the values of the coupling constants "J_{P-H}" and "J_{P-C}" of the second-order multiplets of the PMe_3 ligands refer to the separation between the lines and do not necessarily reflect the true coupling constants.
(9) Crystal data for *trans*-$W(PMe_3)_4(Te)_2$: tetragonal, $I\bar{4}2m$ (No. 121), $a = b = 9.717$ (1) Å, $c = 12.360$ (2) Å, $V = 1167.1$ (3) Å^3, $Z = 2$, ρ_{calcd} = 2.12 g cm^{-3}, μ(Mo Kα) = 80.3 cm^{-1}, λ(Mo Kα) = 0.71073 Å (graphite monochromator); 539 unique reflections with $3° < 2\theta < 60°$ were collected of which 499 reflections with $F > 6\sigma(F)$ were used in refinement; $R = 0.0202$, $R_w = 0.0292$, GOF = 1.136.

0002-7863/91/1513-9421$02.50/0